J. Membrane Biol. 197, 91–99 (2004)
DOI: 10.1007/s00232-003-0644-9

The Journal of
Membrane
Biology

Modulation of DMT1 Activity by Redox Compounds

P. Marciani[1,2], **D. Trotti**[2]*, **M.A. Hediger**[2], **G. Monticelli**[1]
[1]Institute of General Physiology and Biological Chemistry, Pharmacology Faculty, University of Milan, 20134 Milan, Italy
[2]Membrane Biology Program and Renal Division, Brigham and Women's Hospital, Harvard Medical School, Boston, MA 02115, USA

Received: 16 April 2003/Revised: 7 November 2003

Abstract. Iron(II) exacerbates the effects of oxidative stress via the Fenton reaction. A number of human diseases are associated with iron accumulation including ischemia-reperfusion injury, inflammation and certain neurodegenerative diseases. The functional properties and localization in plasma membrane of cells and endosomes suggest an important role for the divalent metal transporter DMT1 (also known as DCT1 and Nramp2) in iron transport and cellular iron homeostasis. Although iron metabolism is strictly controlled and the activity of DMT1 is central in controlling iron homeostasis, no regulatory mechanisms for DMT1 have been so far identified. Our studies show that the activity of DMT1 is modulated by compounds that affect its redox status. We also show that both iron and zinc are transported by DMT1 when expressed in *Xenopus laevis* oocytes. Radiotracer uptake and electrophysiological measurements revealed that H_2O_2 and Hg^{2+} treatments result in substantial inhibition of DMT1. These findings may have a profound relevance from a physiological and pathophysiological standpoint.

Key words: DMT1 — Metal transport — Oxidative stress — Cysteine — Electrophysiology — *Xenopus laevis* oocyte

Introduction

Oxidative stress is a state of imbalance between the production of reactive oxygen species (ROS) and antioxidant mechanisms that leads to oxidation of lipids, proteins, DNA and RNA molecules. ROS are produced within cells by metabolic reactions in physiological conditions as well as in a number of pathological circumstances, such as infectious and inflammatory states (Babior, 1978; McCord, 1987), ischemia-reperfusion (McCord, 1985) or in neurodegenerative disorders such as Parkinson's disease (Dexter et al., 1989; Gerlach et al., 1994). ROS can also be produced and released by phagocytes to affect target cells during immunological response (Fridovich, 1995).

Oxidation of receptor (Aizenman, Hartnett & Reynolds, 1990), channel and transporter proteins (Ruppersberg et al., 1991; Trotti, Danbolt & Volterra, 1998; Trotti et al., 1999) can modulate their activities.

Massive cellular impairment occurs when hydroxyl radicals ($OH^{\bullet}$) are produced from H_2O_2 by the catalytic action of iron (Fe^{2+}) via the Fenton's reaction (Fenton, 1894). Fenton's reaction converts H_2O_2 to the highly toxic $HO^{\bullet}$ radical, and Fe^{2+} acts as a catalytic agent producing a cascade of free radicals. Fe^{3+} can recycle to its reduced state by reducing agents such as ascorbic acid, glutathione or superoxide radicals via the Haber-Weiss reaction:

$$Fe^{2+} + H_2O_2 \rightarrow Fe^{3+} + OH^- + HO^{\bullet}$$

$$Fe^{3+} + O_2^{\bullet -} \rightarrow Fe^{2+} + O_2$$

Hence, excess of iron exacerbates the effect of oxidative stress. Indeed, in ischemia-reperfusion, cell damage can be prevented by administration of iron chelators (van der Kraaij et al., 1988; Omar et al., 1989; Fantini & Yoshioka, 1993). Since increased iron deposition in neurons of the substantia nigra has been reported in Parkinson's disease (PD), iron is thought to play a significant role in selective neuronal loss in PD by oxidative damage (Dexter et al., 1989; Gerlach et al., 1994; Kaur et al., 2003).

Present address for D.T.: Department of Neurology, Cecil B. Day Laboratory for Neuromuscular Research, Massachusetts General Hospital, Harvard Medical School, Charlestown, MA 02129, USA

Correspondence to: G. Monticelli; email: gianluigi.monticelli@unimi.it

In order to minimize these toxic effects of iron, the body as a whole, as well as individual cells, tightly controls iron homeostasis by specific transport mechanisms. In the intestine, uptake into enterocytes takes place directly via the divalent metal transporter, DMT1 (also known as Nramp2 or DCT1) (Gunshin et al., 1997); outside the intestine, iron is taken up by the transferrin receptor-mediated process (Richardson & Ponka, 1997), in which DMT1 participates by transferring iron from the endosomes into the cytoplasm.

DMT1 mediates rapid uptake of Fe^{2+} in both voltage- and pH-dependent fashion. On the basis of electrophysiology measurements DMT1 was supposed to transport divalent cations other than iron, in particular Zn^{2+}, Cd^{2+}, Mn^{2+}, Cu^{2+}, Co^{2+}, Ni^{2+} and Pb^{2+} (Gunshin et al., 1997). Some of these ions are quite toxic to the cell, indicating that DMT1 must have significant toxicological implications. DMT1 is ubiquitously expressed; in the nervous system, it is expressed in neurons, but not in glial or ependymal cells (Gunshin et al., 1997).

DMT1 expression is tightly regulated by body iron requirement, at both the mRNA and protein level (Canonne-Hergaux et al., 1999; Fleming et al., 1999). In the past few years, a regulatory mechanism for iron metabolism in response to oxidative stress has been described (Pantopoulos et al., 1997; Pantopoulos & Hentze, 1998; Brazzolotto et al., 1999). This mechanism is activated by H_2O_2 and involves the interaction between iron regulatory protein 1 (IRP1) and iron responsive elements (IREs) of the mRNAs of numerous proteins involved in iron metabolism (Ponka, Beaumont & Richardson, 1998). Recently, Caltagirone, Weiss and Pantopoulos (2001) demonstrated a modulatory effect of H_2O_2 on iron metabolism. In their study on B6 fibroblasts they found an increase in levels of TfR mRNA and TfR expression on the cell membrane, a reduction of ferritin cell content, at both mRNA and protein level. Interestingly, the DMT1 mRNA level was not affected by hydrogen peroxide treatment.

By means of electrophysiology techniques and radiotracer uptake measurements we investigated the effects of H_2O_2 and Hg^{2+} on the activity of DMT1 expressed in *Xenopus laevis* oocytes.

Materials and Methods

Oocyte Preparation and Microinjection

Xenopus laevis were anaesthetized in 0.1% tricaine methanesulfonate (w/v, pH 7.5). Portions of the ovary were removed and the oocytes harvested by incubation for 2 h at 18°C in 2 mg/ml Collagenase A (Roche) dissolved in Ca^{2+}-free medium (in mM: 88 NaCl, 1 KCl, 2.4 $NaHCO_3$, 0.82 $MgSO_4$, 0.66 $NaNO_3$, 5 HEPES, buffered to pH 7.4 with Tris base). Stage V–VI oocytes were selected, defolliculated and injected with 25 ng/50 nl of capped RNA encoding (wild type) wt-DMT1. Control oocytes were obtained injecting 50 nl of water.

Uptake Measurements

Oocytes were incubated 30 min at room temperature in 250 μl of uptake solution (in mM: 90 NaCl, 1.8 KCl, 0.6 $CaCl_2$, 0.6 $MgCl_2$, 10 HEPES-Na, pH 6.0) containing 20 μM $^{65}Zn^{2+}$ or 10 μM $^{55}Fe^{2+}$ (radioactive chemicals from NEN Life Sciences Products, Boston, MA) plus 1 mM ascorbic acid to keep iron in its divalent form. The specific activity of radioactive tracers was: $^{55}FeCl_2$, 16.94 mCi × mg^{-1}; $^{65}ZnCl_2$, 3.46 mCi × mg^{-1}. The radioactive tracers were not mixed with unlabelled metal ion. Uptake was stopped by washing with cold uptake solution. $^{65}Zn^{2+}$ uptake was assessed by directly counting the zinc content of the oocytes (1282 Compugamma Pharmacia LKB Nuclear, Turku, Finland). For the assessment of oocyte $^{55}Fe^{2+}$ content, oocytes were dissolved in 10% SDS and counted for radioactivity (Tricarb 2200Ca Packard Instrument, Meridan, CT).

Electrophysiological Experiments

Oocytes were mounted in a small recording chamber (100 μl volume) and continuously superfused (5 ml/min) with test solutions. The solute composition of control superfusate (ND96) was in mM: 96 NaCl, 1.8 KCl, 0.6 $CaCl_2$, 0.6 $MgCl_2$, 10 HEPES-Na; pH 6.0.

Two-electrode voltage-clamp recordings were performed at room temperature (20–23°C) using Clampator-1B (Dagan Corp. Minneapolis). Microelectrodes were filled with 3 M KCl and had a tip resistance of 0.5–2 MΩ. Currents were measured at a holding potential (V_h) of −30 or −50 mV. Current-voltage (*I-V*) curves were generated by stepping for 300 ms from the holding potential to potentials (V_m) ranging between −100 and −10 mV in 10 mV increments. The current output was low-pass filtered at 1 kHz. Data generation, acquisition and analysis were carried out with pClamp 8.0 software package (Axon Instruments, Foster City, CA).

Solutions of H_2O_2 and dithiothreitol (DTT) were freshly prepared just before use and perfused at their final concentration. The agents were then washed out for 30 s before measuring zinc-evoked inward currents. The currents were generated adding 50 μM $ZnCl_2$ to the perfusing solution.

In the experiments involving injection of H_2O_2 into oocytes, 9.2 or 23.0 nl of 100 mM hydrogen peroxide in 50 mM K-phosphate buffer, pH 7.4 were delivered by a nano-injector (Automatic injector, Drumond, Broomall, PA). Input resistance of the oocyte membrane was monitored before and after H_2O_2 injection. Hg ions were added to the perfusing medium in their chloride form.

Data Analysis

In electrophysiology experiments steady-state data (obtained by averaging the points over the final 100 ms at each V_m) were fitted to equation:

$$I = \frac{I_{max}[Me^{2+}]^{n_H}}{(K_{0.5})^{n_H} + [Me^{2+}]^{n_H}} \quad (1)$$

for which I is the evoked current (that is, the difference in steady-state current measured in the presence and absence of metal ions Me^{2+}; I_{max}, the derived current maximum; [Me^{2+}], the divalent cation concentration; $K_{0.5}$, the metal concentration at which current was half-maximal; and n_H, the Hill coefficient.

Data are expressed as the mean ± SEM, unless otherwise specified. Statistical analysis was carried out employing either Student's unpaired *t*-test when comparing two data sets or a one-way

Table 1. Rates of uptake of $^{65}Zn^{2+}$ and $^{55}Fe^{2+}$ into *Xenopus laevis* oocytes expressing DMT1

Me^{2+}	$[Me^{2+}]_e$ μM	*t* min	Control pmol oocyte^{-1} t^{-1}	DMT1 pmol oocyte^{-1} t^{-1}	$\Delta[Me^{2+}]_i$ μM	*P*
Fe^{2+}	10	30	0.1 ± 0.0 (9)	29.1 ± 1.7 (9)	58.3 ± 3.5 (9)	<0.01
Zn^{2+}	20	30	0.2 ± 0.0 (10)	11.2 ± 0.8 (7)	22.3 ± 1.5 (7)	ns
Fe^{2+}	10	45	0.2 ± 0.0 (5)	52.9 ± 1.6 (4)	105.8 ± 3.2 (4)	<0.01
Zn^{2+}	20	45	0.5 ± 0.0 (5)	29.1 ± 4.2 (4)	58.1 ± 8.4 (4)	<0.01

Oocytes were from two different batches. Oocytes from the same batch were incubated *t* minutes at room temperature in 250 μl uptake solution (*see* Methods). The rates of uptake of both Zn^{2+} and Fe^{2+} into DMT1-expressing oocytes were significantly greater than into water-injected controls ($P < 0.01$). Assuming an oocyte volume of 500 nl, the uptakes of Zn^{2+} and Fe^{2+} at the rates measured potentially lead to an increase in intracellular metal concentrations $\Delta[Me^{2+}]_i$ at *t*. Comparison of the calculated $\Delta[Me^{2+}]_i$ with the extracellular metal concentrations during uptake experiments, $[Me^{2+}]_e$, indicate intracellular accumulation of metals (*see P*). Data are means ± SEM of the tested oocytes (number of oocytes in parentheses).

analysis of variance when comparing multiple data sets. Differences were considered significant at $P < 0.05$.

Results

DMT1-mediated $^{55}Fe^{2+}$ and $^{65}Zn^{2+}$ Uptake

Fe^{2+} is a redox-active and unstable cation that tends to be oxidized to Fe(III). Therefore, during our uptake studies we kept it in its reduced state by including in the uptake solution 1 mM ascorbic acid.

As shown in Table 1, after 45 min incubation with 10 μM $^{55}Fe^{2+}$ or 20 μM $^{65}Zn^{2+}$, the radioactivity taken up by oocytes expressing DMT1 was consistently higher than in control oocytes, respectively, about 294- and 61-fold. Another batch of oocytes, after 30 min incubation, gave about 246- and 55-fold uptake, respectively, for $^{55}Fe^{2+}$ and $^{65}Zn^{2+}$. We therefore concluded that Zn efficiently and satisfactorily substituted Fe(II) as a substrate for DMT1. This allowed us to use Zn^{2+} rather than Fe^{2+} to study the redox modulation of DMT1 activity and to avoid the presence of ascorbic acid in the uptake solution.

Concentration Dependence of the Zn^{2+}-evoked Currents

When an oocyte expressing DMT1 was voltage-clamped to a negative potential, externally applied Zn^{2+} induced an inward current (Fig. 1*a*; pH 6.0).

At any given Zn^{2+} concentration the induced current was smaller at higher pH_{out} (Fig. 1*b*; pH 7.4).

No significant responses were observed in control water-injected oocytes when external Zn^{2+} was in the range 5–150 μM (*not shown*).

Typical steady-state current-voltage curves in the absence and presence of external Zn^{2+} are shown in Fig. 1*c*.

The magnitude of the Zn-evoked current depended on the membrane potential (V_m) as well as the metal concentration (Fig. 2). A typical current-voltage relationship for the Zn-induced current shows a

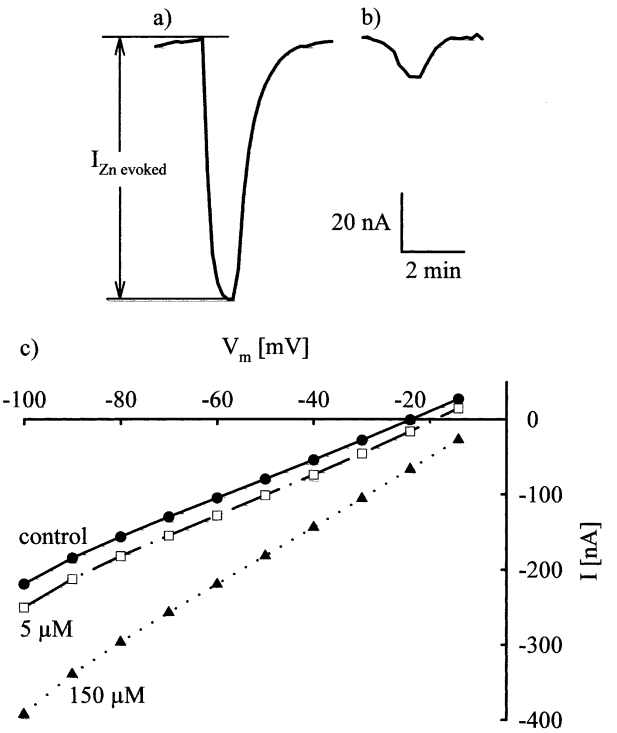

Fig. 1. Representative Zn^{2+}-evoked currents associated with the divalent cation transporter DMT1 expressed in oocytes. (*a*) Current was continuously monitored in a single oocyte expressing DMT1, clamped at −50 mV and superfused at pH 6.0. Zinc (50 μM) was applied for the period shown by the solid bar, then washed out with Zn-free solution. (*b*) As in (*a*) but pH 7.4. (*c*) Typical steady-state current-voltage curves from the same oocyte expressing DMT1 in the absence (*control*) and presence of the indicated concentrations of Zn ions; pH 6.0. Oocytes were voltage-clamped at V_h = −30 mV and 300 ms rectangular pulses (from −100 to −10 mV in 10 mV increments) were applied before and after the addition of Zn^{2+}. The curves are representatives of 7 experiments using oocytes from two animals.

near linear dependence of $I_{Zn\text{-}evoked}$ in the physiological range of potentials (−80 to −10 mV).

Saturation was observed when the metal concentration increased, as expected for a transport system with a fixed number of substrate binding sites.

To characterize the dose dependency of activation, the steady-state responses with respect to

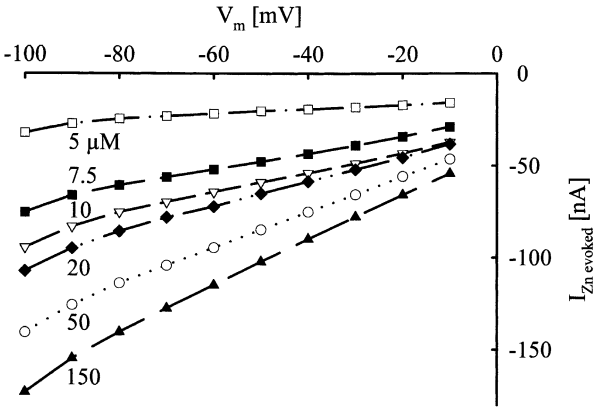

Fig. 2. Voltage- and concentration-dependence of steady-state Zn^{2+}-evoked currents. Zn^{2+}-induced currents were obtained by subtracting the responses in presence of Zn^{2+} ($ZnCl_2$ 5, 7.5, 10, 20, 50 and 150 μM) from the corresponding responses in control solution; pH 6.0. Same representative oocyte as in Fig. 1*c*; $V_h = -30$ mV.

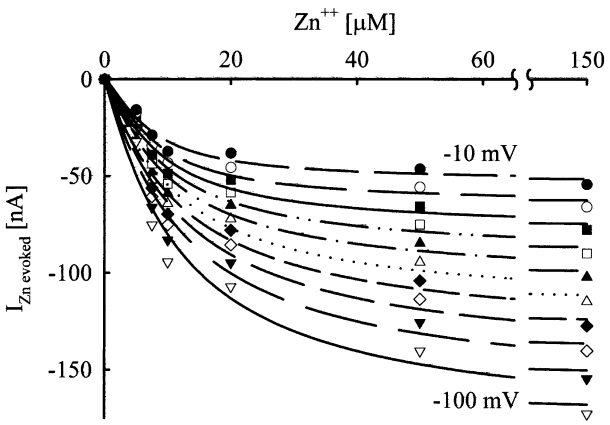

Fig. 3. Concentration-dependence of steady-state Zn^{2+}-evoked inward current into *Xenopus laevis* oocytes expressing DMT1. Oocytes were voltage-clamped at different membrane potentials V_m (from −10 mV to −100 mV in 10 mV increments) and each curve is a three-parameter Hill fit at the respective V_m. Same representative oocyte as in Fig. 2; $V_h = -30$ mV, pH 6.0.

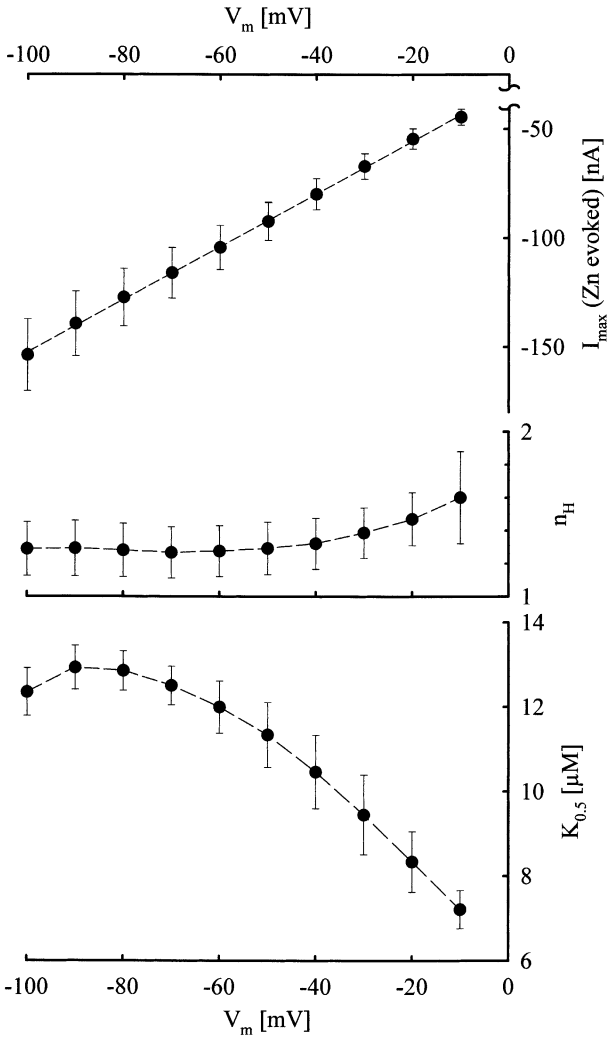

Fig. 4. Voltage-dependence of I_{max} (Zn-evoked), $K_{0.5}$ and n_H, as obtained by fitting to equation (1) the currents evoked by 5, 7.5, 10, 20, 50 and 150 μM $ZnCl_2$. The significance levels resulting from one-way analysis of variance within membrane voltage were $P < 0.01$ for I_{max} and $K_{0.5}$, not significant for n_H. Values are means ± SEM ($n = 7$). $V_h = -30$ mV, pH 6.0.

changing Zn^{2+} concentration at a given membrane potential were fitted with a three-parameter Hill equation (Fig. 3).

Kinetic parameters, I_{max} (Zn-evoked), n_H and $K_{0.5}$, from seven oocytes are plotted against the membrane potential in Fig. 4. The significance levels resulting from one-way analysis of variance within membrane voltage were $P < 0.01$ for I_{max} and $K_{0.5}$, not significant for n_H.

Effect of H_2O_2 Addition on the Zn^{2+} Transport

The effect of extracellular H_2O_2 on the $^{65}Zn^{2+}$ uptake was studied as a function of H_2O_2 concentration (0.05, 0.1, 0.2, 0.4, 1 mM). Following 3 h preincubation in H_2O_2 and 30 min in uptake solution containing 20 μM $^{65}Zn^{2+}$, we obtained the results reported in Fig. 5. DMT1-mediated $^{65}Zn^{2+}$ uptake was affected by extracellular application of H_2O_2 in a dose-dependent fashion. $^{65}Zn^{2+}$ uptake, as % of control, was fitted to a three-parameter logistic equation; $\log(IC_{50})$ resulted in -4.08 ± 0.03 ($n = 38$ oocytes), $IC_{50} = 83.2$ μM.

In voltage-clamp experiments ($V_h = -50$ mV) the injection of H_2O_2 (2 or 5 mM, initial intracellular concentration calculated assuming an oocyte volume of 500 nl) into oocytes expressing DMT1 did not affect the Zn^{2+}-evoked currents (Fig. 6*a* and 6*b*).

In experiments like the one reported in Fig. 6*a* we surely missed an H_2O_2 effect because of an insufficient

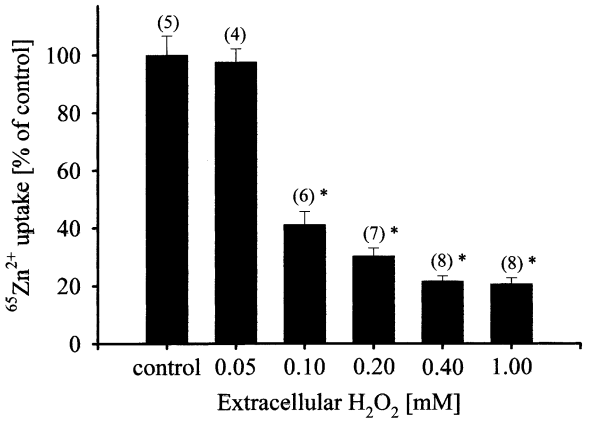

Fig. 5. Dose-dependent inhibition of $^{65}Zn^{2+}$ uptake by hydrogen peroxide into *Xenopus laevis* oocytes expressing DMT1. $^{65}Zn^{2+}$ uptake assays were performed on 38 oocytes from the same batch following 3 h preincubation in H_2O_2 and further incubated for 30 min in uptake solution containing 20 μM $^{65}Zn^{2+}$. Data are means ± SEM of the tested oocytes (numbers in parentheses). *:$P < 0.01$, indicating significant difference in zinc uptake at the indicated H_2O_2 concentrations compared with control oocytes. $^{65}Zn^{2+}$ uptakes, as % of control, were fitted to a three-parameter logistic equation; $\log(IC_{50})$ resulted in -4.08 ± 0.03 ($n = 38$), $IC_{50} = 83.2$ μM.

H_2O_2 concentration and of the large time lag to induce currents by Zn^{2+} application.

No effects were observed when the H_2O_2 initial intracellular concentration was 5 mM and Zn^{2+} applied 30 s after H_2O_2 injection. A new injection of H_2O_2, 6 min from the previous one, did not alter the Zn^{2+}-evoked currents (Fig. 6*b*).

In contrast, H_2O_2 5 mM reduced Zn^{2+}-evoked currents about 40% when added to the bathing solution. This inhibition was reversed by application of the reducing agent DTT 2 mM (Fig. 6*c*).

Effects of the Hydrophilic Sulfhydryl-chelating Agent Hg^{2+} on DMT1

Hg^{2+} is a specific thiol-reactive compound that is capable of coordinated ligation of two cysteinyl residues (S-Hg-S) or of coordinated binding to a single cysteine residue (S-Hg^{+}).

As shown in Fig. 7, exposure of an oocyte expressing DMT1 to a 1 μM Hg^{2+}-containing solution induced a slow inward current to maintain $V_h = -50$ mV. After superfusion with 1 μM Hg^{2+}-containing solution, the Zn^{2+}-evoked current, in the absence of Hg^{2+}, was inhibited by 41.1 ± 2.7% ($n = 13$; 5 oocytes). Simple washout did not restore the initial holding current. The increased holding and the reduced Zn^{2+}-evoked currents were stable after Hg^{2+} treatment in the absence of a reducing agent.

DMT1 activity was slowly restored by extracellular application of the specific disulfide reducing agent DTT (2 mM).

After Hg^{2+} treatment, the magnitude of the Zn-evoked current continued to depend on the membrane potential (V_m) as well as on the metal concentrations. Typical steady-state responses with respect to changing Zn^{2+} concentration at a given membrane potential are reported in Fig. 8.

Data from two oocytes after 20 min superfusion with 1 μM Hg^{2+} were analyzed using equation 1. At any given V_m (−100 to −10 mV) the calculations revealed that: 1) I_{max} (Zn-evoked) was always lower than before Hg^{2+} treatment; 2) $K_{0.5}$ did not vary appreciably and resulted in 5.0 ± 0.0 and 5.5 ± 0.1 μM ($n = 10$ voltages), lower than before Hg^{2+} treatment (Fig. 4); 3) n_H values did not change significantly in individual experiments but the two oocytes gave different values, 7.5 ± 0.2 and 3.9 ± 0.1 ($n = 10$), both higher values than in control oocytes (Fig. 4).

Discussion

The capability of the cell iron transfer system to adapt to iron content is of great importance to preserve homeostasis of iron because regulation through secretion is not possible.

The divalent metal transporter DMT1 may represent a key mediator of iron absorption. It is a 561-amino-acid protein with 12 putative membrane-spanning domains, and it has been found ubiquitously expressed (Gunshin et al., 1997). At least two isoforms of DMT1, resulting from alternative splicing, were identified and shown to have different cellular localization (Gruenheid et al., 1995; Fleming et al., 1998; Lee et al., 1998; Rolfs et al., 2002). Hubert and Henze (2002) recently showed the existence of four DMT1 isoforms with at least two iron regulatory regions, one being the IRE-containing 3′ UTR exon and the other is defined by the presence of exon 1A. The two regulatory regions seem to be used in different ways in distinct tissues and, at subcellular levels, these isoproteins could localize depending on the N and/or C terminus as well as differ in their metal selectivity and/or transport capacity.

However, under oxidative stress conditions, as produced by oxidative metabolism in which energy activation and electron reduction are involved, a direct cellular mechanism to regulate DMT1 activity would be beneficial to cells to prevent excessive iron uptake.

The balance between free radical production and antioxidant defenses determines the degree of oxidative stress (Finkel & Holbrook, 2000). Fe^{2+} is a redox-active cation. During uptake studies ascorbic acid must be added to the solutions to maintain iron

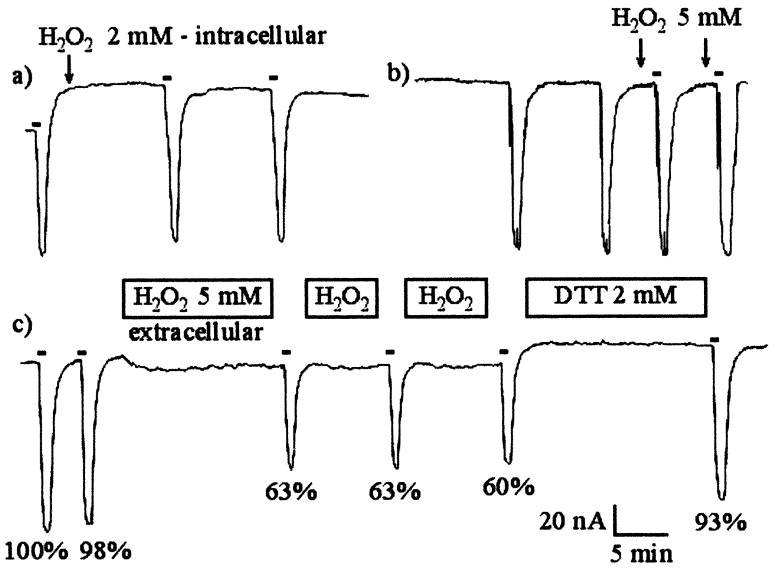

Fig. 6. Effect of H_2O_2 on Zn^{2+}-induced DMT1-mediated current. DMT1 cRNA-injected oocytes were superfused (ND96, pH 6.0) and voltage-clamped (V_h = −50 mV). The injection (time indicated by the arrow) of H_2O_2 (2 or 5 mM, intracellular concentration) into oocytes did not affect the Zn^{2+}-evoked currents (*a, b*). For a number of reasons (*see* Discussion section), in experiments like the one shown in (*a*), the possible effect of H_2O_2 was surely missed because of its low concentration and of the time lag to Zn^{2+} application (50 μM Zn^{2+}; *black dash*). No effects were observed either when the H_2O_2 intracellular concentration was 5 mM and Zn^{2+} applied 30 s after H_2O_2 injection. New injections of H_2O_2 (6 min from the previous one in *b*) did not alter the Zn^{2+}-evoked currents. In contrast, H_2O_2 5 mM reduced Zn^{2+}-evoked currents about 40% when added to the bathing solution; 2 mM DTT fully recovered DMT1 activity. Zinc-activated currents were obtained applying Zn^{2+} after 30 s washout of redox reagents (*c*). Percentage of activation is given for each Zn^{2+}-evoked current peak.

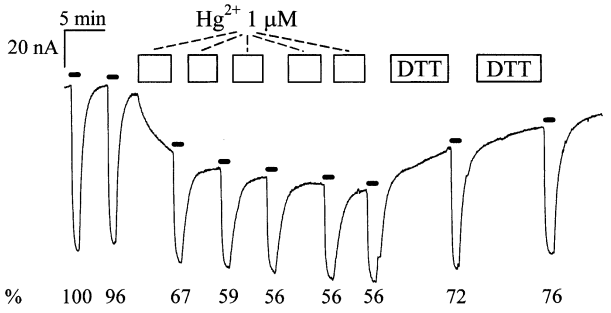

Fig. 7. Susceptibility of DMT1 to Hg^{2+}. Representative recordings of zinc-activated currents. Wild-type DMTl-cRNAs 25 ng were injected into oocytes and Zn^{2+}-induced currents were measured under voltage-clamp conditions (V_h, = −50 mV). 1 μM Hg^{2+} (empty boxes) and 2 mM DTT were applied in control superfusate; during Hg^{2+} and DTT treatment, 50 μM Zn^{2+} (*black dashes*) was given after a brief washout. Percentage of control maximal activation (calculated with respect to the average of the peak values before Hg^{2+} treatment) is indicated at the bottom of each Zn-evoked current peak.

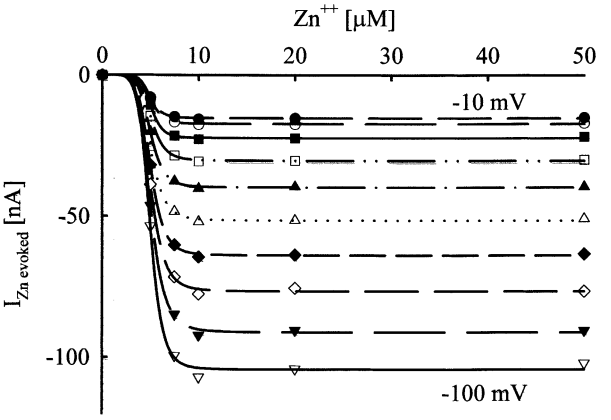

Fig. 8. Concentration-dependence of the steady-state Zn^{2+}-evoked current after Hg^{2+} treatment. Oocytes expressing DMT1 were voltage-clamped at different membrane potentials V_m (from −10 mV to −100 mV in 10 mV increments) and each curve is a three-parameter Hill fit at the respective V_m. Same representative oocyte as in Fig. 3 after 20 min superfusion with 1 μM Hg^{2+} (V_h = −30 mV, pH 6.0). Currents were measured in the absence of Hg ions.

in ferrous form. However, such a reductant would interfere with redox compounds used in the present research. Thus, Fe^{2+} would have been inappropriate to study the effect of oxidative alterations of DMT1.

Our data show that DMT1 transports Zn^{2+} as well as Fe^{2+} (Table 1). Even though Zn^{2+} uptake by DMT1 was smaller than Fe^{2+} uptake, we took advantage of this result, using Zn^{2+} (which does not interfere with redox compounds) rather than Fe^{2+} to study DMT1 modulation by redox compounds. Assuming an oocyte volume of 500 nl, the uptake of Fe^{2+} and Zn^{2+} at the measured rates would potentially lead to an increase in intracellular metal concentration, $\Delta[Me^{2+}]_i$, as summarized in Table 1. In DMT1-expressing oocytes both Fe^{2+} and Zn^{2+} uptakes appear to be accumulative. Zn^{2+} intra- and extracellular concentrations were at equilibrium in uptake experiments and followed for 30 min (*ns* in Table 1). Intracellular metal ions, however, are protein-bound and the calculated concentrations must be considered an overestimate.

This is the first direct documentation of Zn^{2+} transport by DMT1 and confirms the previous speculation based on measuring Zn^{2+}-evoked currents in oocytes expressing DMT1 (Gunshin et al., 1997). Recently Sacher, Cohen & Nelson (2001) reported

that there is no detectable transport of $^{65}Zn^{2+}$ into *Xenopus laevis* oocytes expressing DMT1 and the elevation of the concentration from 0.5 to 10 μM had no detectable effect on uptake activity. We have to consider the following: 1) in our uptake experiments we used $^{65}ZnCl_2$ (20 μM) without mixing radioactive tracer with unlabelled metal ion; 2) in two different batches, working at pH_{out} 6.0 in NaCl medium, we measured ^{55}Fe uptake of 52.9 ± 1.6 (n = 4 oocytes) and 29.1 ± 1.7 (n = 9) pmol per oocyte, respectively, over 45 and 30 min, compared with about 27.4 ± 8.2 pmol h^{-1} $oocyte^{-1}$ (in choline chloride medium, pH 5.5; Sacher, Cohen & Nelson, 2001); Gunshin et al. (1997) reported 88 ± 12 pmol over 1.5 h per oocyte at pH 6.2 in NaCl medium; 3) in voltage-clamp experiments (V_h = −50 mV) we observed large inward currents (100 − 120 nA) when 50 μM Zn^{2+} were added to the bathing solution; Gunshin et al. (1997) reported a similar value (∼122 nA), Sacher et al. (2001; V_h not indicated) ∼91 nA adding 1 mM $ZnCl_2$; all measurements were performed at pH 5.5 in NaCl medium. The rate of uptake and the currents are related to the number of transporters expressed in the membrane; the above observations could be accounted for by a low expression of DMT1 in experiments of Sacher et al. (2001).

Our data are in agreement with the observation of a divalent cation transporter in small intestine BBMV (Knopfel et al., 2000); the authors report a pH dependence of Zn^{2+} transport and kinetic parameters resembling DTM1 characteristics. These findings have not been confirmed in a recent study on Caco-2 cells. Nevertheless, as the same authors suggest, "...high levels of DMT1 are needed for the DMT1-mediated transport of lead and zinc, Caco-2 cells rather express low levels of DMT1 but express other transporters in sufficient amounts to transport lead and zinc" (Bannon et al., 2003).

The magnitude of the Zn-evoked current depended on the membrane potential as well as the metal concentrations (Fig. 2) and, at a given membrane potential, saturation was observed when $[Zn^{2+}]_{out}$ increased, as expected for a transport system with a fixed number of substrate binding sites. Kinetic parameters, I_{max} (Zn-evoked) and $K_{0.5}$, were dependent on the membrane voltage, whereas n_H was not.

H_2O_2 induces protein thiol oxidation. Oxidation of SH- groups by H_2O_2 (van Iwaarden, Driessen & Konings, 1992) results in the formation of inter- or intramolecular disulfide bonds $2R\text{-}SH \leftrightarrow R\text{-}S\text{-}S\text{-}R + 2H^+ + 2e^-$ and/or other compounds. Zinc uptake progressively decreases with increasing hydrogen peroxide concentration (Fig. 5). The concentration-response curve has a baseline response at about 20% of the control and a Hill slope of −5.3; the resulting IC_{50} was 83.2 μM.

The dose response for hydrogen peroxide inhibition of radioactive tracer uptake (Fig. 5) appears quite different from that of intracellularly injected (∼2 or 5 mM) or externally applied (5 mM) H_2O_2 effects on Zn-evoked currents (Fig. 6). Application of 5 mM H_2O_2 only suppresses ∼40% activity, but based on an IC_{50} of 83.2 μM, metal transport should be entirely blocked at the baseline value. Arguments accounting for this discrepancy could be: 1) the voltage dependence of the metal-evoked currents (Gunshin et al., 1997)—only in electrophysiological experiments the membrane voltage was controlled; 2) the time of exposure to H_2O_2 was very different in uptake and electrophysiological experiments.

Injection of H_2O_2 into voltage-clamped oocytes expressing DMT1 did not affect holding currents, while a small increment of I_h (∼10 nA) has been observed when oxidant has been given in the bathing solution. This finding is not in disagreement with data reported by Kim & Han (2001), since our experiments were performed more than three days after *Xenopus* surgery.

Even though H_2O_2 is a permeant molecule, H_2O_2 did not affect Zn-evoked current when added (∼5 mM) to the intracellular side (Fig. 6*b*), whereas H_2O_2 in the bathing solution has been shown to inhibit the Zn-generated current by about 40% (Fig. 6*c*). Incubation in 2 mM DTT, a specific hydrophilic thiol reductant (van Iwaarden et al., 1992), restored the Zn^{2+}-activated currents, suggesting a redox-sensing region within the transporter protein.

It is not surprising that H_2O_2 was ineffective when intracellularly injected (∼2 mM, Fig. 6*a*); its large membrane permeability coefficient ($\sim 10^{-4}$ cm × s^{-1}), the small intracellular volume (∼500 nl) and the activity of H_2O_2-removing enzymes account for rapid emptying of cell H_2O_2, before Zn^{2+} application. Then we increased H_2O_2 intracellular concentration to 5 mM (Fig. 6*b*) and applied Zn^{2+} 30 s after H_2O_2 injection. Zn^{2+}-evoked current was not affected. A new injection of H_2O_2, 6 min after the previous one, was ineffective too. In these conditions, neglecting solute metabolization as well as a rapid turnover of injected H_2O_2 by catalases or other H_2O_2-removing enzymes and simply considering diffusion through the membrane, the half-time for equilibration is 114 s and the intracellular actual concentrations of H_2O_2, at the time of current measurements (30 s after H_2O_2 injection), would be 4.2 and 4.6 mM respectively.

Our study shows that the transport activity of the divalent metal transporter DMT1 is inhibited (−41.1 ± 2.7%) by thiol- reactive agents such as Hg^{2+}. It is conceivable that similar to Zn^{2+}, Hg^{2+} is actually transported by DMT1 and that it exerts its action on thiol (SH) groups located at the inner surface of the protein. DMT1 function was rescued after incubation with DTT (Fig. 7).

Hg^{2+} is an environmental toxicant and H_2O_2 is an oxidant formed in vivo during biological processes. It reaches higher concentration under

conditions of oxidative stress, which is enhanced in the presence of free iron due to $OH^{\bullet}$ production (Stadtman, 1993; Jellinger, 1999).

Under physiological conditions, iron metabolism is tightly regulated and iron accumulation is associated with oxidative damage in some pathologies (Gerlach et al., 1994). H_2O_2 production in cells is a normal physiological process; despite its toxicity, H_2O_2 can act as a second messenger in glial and neuronal function (Finkel, 1998; Kaltschmidt, Sparna & Kaltschmidt, 1999). We suggest DMT1 inhibition by hydrogen peroxide to be part of these defensive mechanisms; DMT1 molecule would sense the oxidative state of cell environment and modulate iron intake in order to avoid the catalysis of radical production.

Although several amino-acid residues are sensitive to oxidative agents, a number of proteins, among them transporters, channels and receptors (Aizenman et al., 1990; Ruppersberg et al., 1991; Trotti et al., 1997a, 1997b, 1999) exhibit redox modulation involving sensitivity of reactive cysteine residues. The evidence that Hg^{2+} inhibits the transport activity of DMT1 together with the protective action of the reductant dithiotreitol points towards the involvement of cysteine residues.

Massive ROS production occurs in a broad spectrum of pathological situations, such as infectious (Babior, 1978) and inflammatory diseases (McCord, 1987), and in all the pathologies that cause ischemia and reperfusion (McCord, 1985). Under these circumstances, the oxidative burst of circulating neutrophils and macrophages leads to the production of reactive oxygen intermediates and to the increase of extracellular H_2O_2 (Thannickal & Fanburg, 1995). It is worth noting here that this production of active oxygen intermediates depends upon the availability of transition metal ions, especially iron and manganese, and that DMT1 localizes in macrophages (Goswami, Rolfs & Hediger, 2002). Moreover, iron overload and oxidative damage colocalize in Parkinsonian neurons (Dexter et al., 1989; Gerlach et al., 1994).

Little is known about the mechanism of iron accumulation in specific regions of the brain affected in neurodegenerative diseases (e.g., Parkinson's and Alzheimer's diseases). In addition to the Tfr-mediated pathway (Qian, Pu & Wang, 1998), Qian et al. (1999) provided some evidence for the presence of membrane iron carrier-mediated transport in the cultured cerebellar granule cells in rats; the ion selectivity of the transporter resembled that of DMT1. In agreement with these findings, the transferrin receptor expression was not increased in substantia nigra of Parkinsonian rats, indicating that the TfR-mediated process may not be involved in iron accumulation in Parkinsonian neurons (He, Lee & Leong, 1999).

Recently, the involvement of iron and the beneficial effect of iron chelation has been demonstrated in a Parkinsonian animal model (Kaur et al., 2003). The brain iron content is reduced in Belgrade rats as a result of the inactivating G185R DMT1 mutation, indicating that DMT1 is an important component of the iron transport system in the brain (Burdo et al., 1999). In situ hybridization and immunocytochemistry of rat brains revealed that DMT1 is expressed in neurons throughout the CNS (Gunshin et al., 1997; Burdo et al., 2001).

In conclusion, our data indicate a possible inhibitory regulation of iron uptake involving DMT1, which could be part of a defensive mechanism to protect cells from oxidative injury in oxidative stress-associated pathologies. However, whether and to what extent such inhibition is important in pathological situations remains to be determined.

References

Aizenman, E., Hartnett, K.A., Reynolds, I.J. 1990. Oxygen free radicals regulate NMDA receptor function via a redox modulatory site. *Neuron* **5:**841–846

Babior, B.M. 1978. Oxygen-dependent microbial killing by phagocytes (first of two parts). *N. Engl. J. Med.* **298:**659–668

Bannon, D.I., Abounader, R., Lees, P.S.J., Bressler, J.P. 2003. Effect of DMT1 knockdown on iron, cadmium and lead uptake in Caco-2 cells. *Am. J. Physiol.* **28:**C44–C50

Brazzolotto, X., Gaillard, J., Pantopoulos, K., Hentze, M.W., Moulis, J.M. 1999. Human cytoplasmic aconitase (Iron regulatory protein 1) is converted into its [3Fe-4S] form by hydrogen peroxide in vitro but is not activated for iron-responsive element binding. *J. Biol Chem.* **274:**21625–21630

Burdo, J.R., Martin, J., Menzies, S.L., Dolan, K.G., Romano, M.A., Fletcher, R.J., Garrick, M.D., Garrick, L.M., Connor, J.R. 1999. Cellular distribution of iron in the brain of the Belgrade rat. *Neuroscience* **93:**1189–1196

Burdo, J.R., Menzies, S.L., Simpson, I.A., Garrick, L.M., Garrick, M.D., Dolan, K.G., Haile, D.J., Beard, J.L., Connor, J.R. 2001. Distribution of divalent metal transporter 1 and metal transport protein 1 in the normal and Belgrade rat. *J. Neurosci. Res.* **66:**1198–1207

Caltagirone, A., Weiss, G., Pantopoulos, K. 2001. Modulation of cellular iron metabolism by hydrogen peroxide. Effects of H_2O_2 on the expression and function of iron-responsive element-containing mRNAs in B6 fibroblasts. *J. Biol Chem.* **276:**19738–19745

Canonne-Hergaux, F., Gruenheid, S., Ponka, P., Gros, P. 1999. Cellular and subcellular localization of the Nramp2 iron transporter in the intestinal brush border and regulation by dietary iron. *Blood* **93:**4406–4417

Dexter, D.T., Wells, F.R., Lees, A.J., Agid, F., Agid, Y., Jenner, P., Marsden, C.D. 1989. Increased nigral iron content and alterations in other metal ions occurring in brain in Parkinson's disease. *J. Neurochem.* **52:**1830–1836

Fantini, G.A., Yoshioka, T. 1993. Deferoxamine prevents lipid peroxidation and attenuates reoxygenation injury in postischemic skeletal muscle. *Am. J. Physiol* **264:**H1953–H1959

Fenton, H.J.H. 1894. Oxidation of malic acid by hydrogen peroxide. *J. Chem. Soc.* (*Lond.*) **65:**899–910

Finkel, T. 1998. Oxygen radicals and signaling. *Curr. Opin. Cell Biol* **10:**248–253

Finkel, T., Holbrook, N.J. 2000. Oxidants, oxidative stress and the biology of ageing. *Nature* **408:**239–247

Fleming, R.E., Migas, M.C., Zhou, X., Jiang, J., Britton, R.S., Brunt, E.M., Tomatsu, S., Waheed, A., Bacon, B.R., Sly, W.S. 1999. Mechanism of increased iron absorption in murine model of hereditary hemochromatosis: increased duodenal expression of the iron transporter DMT1. *Proc. Natl. Acad. Sci. U.S.A* **96:**3143–3148

Fleming, M.D., Romano, M.A., Su, M.A., Garrick, L.M., Garrick, M.D., Andrews, N.C. 1998. Nramp2 is mutated in the anemic Belgrade (b) rat: evidence of a role for Nramp2 in endosomal iron transport. *Proc. Natl. Acad. Sci. USA* **95:**1148–1153

Fridovich, I. 1995. Superoxide radical and superoxide dismutases. *Annu. Rev. Biochem.* **64:**97–112

Gerlach, M., Ben Shachar, D., Riederer, P., Youdim, M.B. 1994. Altered brain metabolism of iron as a cause of neurodegenerative diseases? *J. Neurochem.* **63:**793–807

Goswami, T., Rolfs, A., Hediger, M.A. 2002. Iron transport: emerging roles in health and disease. *Biochem. Cell Biol* **80:**679–689

Gruenheid, S., Cellier, M., Vidal, S., Gros, P. 1995. Identification and characterization of a second mouse Nramp gene. *Genomics* **25:**514–525

Gunshin, H., Mackenzie, B., Berger, U.V., Gunshin, Y., Romero, M.F., Boron, W.F., Nussberger, S., Gollan, J.L., Hediger, M.A. 1997. Cloning and characterization of a mammalian proton-coupled metal-ion transporter. *Nature* **388:**482–488

He, Y., Lee, T., Leong, S.K. 1999. Time-course and localization of transferrin receptor expression in the substantia nigra of 6-hydroxydopamine-induced parkinsonian rats. *Neuroscience* **91:** 579–585

Hubert, N., Hentze, M.W. 2002. Previously uncharacterized isoforms of divalent metal transporter (DMT)-1: implications for regulation and cellular function. *Proc. Natl. Acad. Sci. USA* **99:**12345–12350

Jellinger, K.A. 1999. The role of iron in neurodegeneration: prospects for pharmacotherapy of Parkinson's disease. *Drugs Aging* **14:**115–140

Kaltschmidt, B., Sparna, T., Kaltschmidt, C. 1999. Activation of NF-kappa B by reactive oxygen intermediates in the nervous system. *Antioxid. Redox. Signal.* **1:**129–144

Kaur, D., Yantiri, F., Rajagopalan, S., Kumar, J., Mo, J.Q., Boonplueang, R., Viswanath, V., Jacobs, R., Yang, L., Beal, M.F., DiMonte, D., Volitaskis, I., Ellerby, L., Cherny, R.A., Bush, A.I., Andersen, J.K. 2003. Genetic or pharmacological iron chelation prevents MPTP-induced neurotoxicity *in vivo:* a novel therapy for Parkinson's disease. *Neuron* **37:**899–909

Kim, M.-J., Han, J.-K. 2002. Hydrogen peroxide-induced current in *Xenopus* oocytes: current characteristics similar to those induced by the removal of extracellular calcium. *Biochem. Pharmacol.* **63:**569–576

Knopfel, M., Schulthess, G., Funk, F., Hauser, H. 2000. Characterization of an integral protein of the brush border membrane mediating the transport of divalent metal ions. *Biophys. J.* **79:**874–884

Lee, P.L., Gelbart, T., West, C., Halloran, C., Beutler, E. 1998. The human Nramp2 gene: characterization of the gene structure, alternative splicing, promoter region and polymorphisms. *Blood Cells Mol. Dis.* **24:**199–215

McCord, J.M. 1985. Oxygen-derived free radicals in postischemic tissue injury. *N. Engl. J. Med.* **312:**159–163

McCord, J.M. 1987. Oxygen-derived radicals: a link between reperfusion injury and inflammation. *Fed. Proc.* **46:**2402–2406

Omar, R., Nomikos, I., Piccorelli, G., Savino, J., Agarwal, N. 1989. Prevention of postischaemic lipid peroxidation and liver cell injury by iron chelation. *Gut* **30:**510–514

Pantopoulos, K., Hentze, M.W. 1998. Activation of iron regulatory protein-1 by oxidative stress in vitro. *Proc. Natl. Acad. Sci. U.S.A* **95:**10559–10563

Pantopoulos, K., Mueller, S., Atzberger, A., Ansorge, W., Stremmel, W., Hentze, M.W. 1997. Differences in the regulation of iron regulatory protein-1 (IRP-1) by extra- and intracellular oxidative stress. *J. Biol. Chem.* **272:**9802–9808

Ponka, P., Beaumont, C., Richardson, D.R. 1998. Function and regulation of transferrin and ferritin. *Semin. Hematol.* **35:**35–54

Qian, Z.M., Pu, Y.M., Wang, Q. 1998. Transferrin-bound iron uptake by cerebellar granule cells. *Neurosci. Lett.* **251:**9–12

Qian, Z.M., Pu, Y.M., Wang, Q., Ke, Y., Yao, Y.D., Chen, W.F., Shen, X., Feng, Y.M., Tang, P.L. 1999. Cerebellar granule cells acquire transferrin-free iron by a carrier-mediated process. *Neuroscience* **92:**577–582

Richardson, D.R., Ponka, P. 1997. The molecular mechanisms of the metabolism and transport of iron in normal and neoplastic cells. *Biochim. Biophys. Acta* **1331:**1–40

Rolfs, A., Bonkovsky, H.L., Kohlroser, J.G., McNeal, K., Sharma, A., Berger, U.V., Hediger, M.A. 2002. Intestinal expression of genes involved in iron absorption in humans. *Am. J. Physiol. Gastrointest. Liver Physiol* **282:**G598–G607.

Ruppersberg, J.P., Stocker, M., Pongs, O., Heinemann, S.H., Frank, R., Koenen, M. 1991. Regulation of fast inactivation of cloned mammalian IK(A) channels by cysteine oxidation. *Nature* **352:**711–714

Sacher, A., Cohen, A., Nelson, N. 2001. Properties of the mammalian and yeast metal-ion transporters DCT1 and Smf1p expressed in *Xenopus laevis* oocytes. *J. Exp. Biol* **204:**1053–1061

Stadtman, E.R. 1993. Oxidation of free amino acids and amino acid residues in proteins by radiolysis and by metal-catalyzed reactions. *Annu. Rev. Biochem.* **62:**797–821

Thannickal, V.J., Fanburg, B.L. 1995. Activation of an H_2O_2-generating NADH oxidase in human lung fibroblasts by transforming growth factor beta 1. *J. Biol. Chem.* **270:**30334–30338

Trotti, D., Danbolt, N.C., Volterra, A. 1998. Glutamate transporters are oxidant-vulnerable: a molecular link between oxidative and excitotoxic neurodegeneration? *Trends Pharmacol. Sci.* **19:**328–334

Trotti, D., Nussberger, S., Volterra, A., Hediger, M.A. 1997b. Differential modulation of the uptake currents by redox interconversion of cysteine residues in the human neuronal glutamate transporter EAAC1. *Eur. J. Neurosci.* **9:**2207–2212

Trotti, D., Rizzini, B.L., Rossi, D., Haugeto, O., Racagni, G., Danbolt, N.C., Volterra, A. 1997a. Neuronal and glial glutamate transporters possess an SH-based redox regulatory mechanism. *Eur. J. Neurosci.* **9:**1236–1243

Trotti, D., Rolfs, A., Danbolt, N.C., Brown R.H. Jr., Hediger, M.A. 1999. SOD1 mutants linked to amyotrophic lateral sclerosis selectively inactivate a glial glutamate transporter. *Nat. Neurosci.* **2:**427–433

van der Kraaij, A.M., Mostert, L.J., van Eijk, H.G., Koster, J.F. 1988. Iron-load increases the susceptibility of rat hearts to oxygen reperfusion damage. Protection by the antioxidant (+)-cyanidanol-3 and deferoxamine. *Circulation* **78:**442–449

van Iwaarden, P.R., Driessen, A.J., Konings, W.N. 1992. What we can learn from the effects of thiol reagents on transport proteins. *Biochim. Biophys. Acta* **1113:**161–170